ChemPubSoc Europe

DOI: 10.1002/ejic.201701064

EurJIC European Journal of Inorganic Chemistry

Full Paper

Oxidation Catalysts

Dinuclear Manganese(II), Cobalt(II), and Nickel(II) Aryl Phosphates Incorporating 4′-Chloro-2,2′:6′,2″-Terpyridine Coligands – Efficient Catalysts for Alcohol Oxidation

Gulzar A. Bhat,[a] Antony Rajendran,[a] and Ramaswamy Murugavel*[a]

Dedicated to Prof. K. C. Kumara Swamy on the occasion of his 60th birthday

Abstract: The dinuclear cyclo(metallo)phosphates [M(dipp)(Cl-terpy)]$_2$ [M = Mn (**1**), Ni (**2**)] and the mononuclear cobalt phosphate [Co(dippH)(Cl-terpy)(MeOH)(H_2O)]·dippH (**3**) were synthesized through the reactions of 4′-chloro-2,2′:6′,2″-terpyridine (Cl-terpy) and 2,6-diisopropylphenyl phosphate (dippH$_2$) with manganese, nickel, and cobalt acetates. The formation of **1**–**3** is supported by spectroscopic, thermogravimetric, and microanalytical data. The molecular structures of **1** and **3** were confirmed by single-crystal X-ray diffraction studies. Compounds **1** and **2** are dimeric and feature two octahedral metal centers bridged by dianionic dipp ligands. On the other hand, **3** exists as a monomer in the solid state, but dissolution in methanol converts it to a dimeric form similar to those of **1** and **2**, as evidenced by ESI-MS studies. Compounds **1**–**3** were employed as catalysts for alcohol oxidation reactions with *tert*-butyl hydroperoxide (TBHP) as the oxidant. The manganese phosphate **1** exhibits better catalytic activity in terms of selectivity and substrate conversion compared with those of **2** and **3** under similar conditions.

Introduction

The oxidation of alcohols to carbonyl compounds is a fundamental reaction in organic chemistry and also plays a pivotal role in industries such as pharmaceuticals, agrochemicals, and perfumery.[1] Different catalysts have been employed for such conversions as they offer advantages in terms of high conversions and selectivities, broader substrate scope, and environmental friendliness compared with the use of stoichiometric reagents.[2] Thus, there is great scope for such catalysts, and metal-based catalysts are more desirable in terms of selectivity, productivity, and environmental concerns than other reported catalysts for such reactions.[1c,3] Transition-metal catalysts are particularly attractive owing to their inherent tendency to exist in more than one oxidation state and the availability of vacant d orbitals.[4] Similarly, the use of organic peroxides such as *tert*-butyl hydroperoxide (TBHP) is more favorable than the use of toxic inorganic oxidants ($KMnO_4$ and CrO_3 compounds).[5] Transition-metal catalysts based on Pd, Ru, Au, and Pt complexes have emerged as better catalysts in terms of selectivity and conversion but are limited by their low abundances and subsequent high costs, which limit their use in alcohol oxidation reactions.[1e,2,6] Furthermore, a base is needed to promote Au-catalyzed alcohol oxidations; consequently, the selectivity is reduced owing to the enhanced possibility of the formation of undesirable carboxylates.[7] Thus, catalysts based on first-row transition metals are a better choice owing to their affordability, good selectivity, and adequate activity.

The strong π-acceptor ligand 2,2′:6′,2″-terpyridine (terpy) has been employed widely to generate transition-metal complexes ranging from discrete to polymeric species,[8] owing to its intrinsic ability to tune the nuclearities and geometries of the resulting complexes.[9] Enhanced synthetic routes to terpy and its derivatives along with their rich coordination chemistry have paved the way for the application of such terpy-containing complexes in catalysis and biological systems.[10] Crabtree and co-workers reported the mixed-valent Mn_2(III,IV) "terpy dimer" [Mn(terpy)(H_2O)O]$_2$[NO_3]$_3$, in which the two Mn ions are bridged by two μ-oxygen atoms, as a functional model for the O–O bond formation reactions of the oxygen-evolving complex (OEC) of photosystem II (PS-II).[11] This observation led to the screening of a large number of terpyridine-containing coordination complexes of Mn, Co, and Ru as water oxidation catalysts (WOCs), and the cooperativity between the metal center and the ligand is crucial for catalytic performance.[12] Manganese terpy complexes bridged by oxo groups are excellent WOCs owing to the cooperativity between the Mn ions.[12a,12b,13] The transition-metal complexes of Mn, Co, Ni, and Cu have also been explored as efficient catalysts in alcohol oxidation reactions.[3a,14] Manganese(II)/cobalt(II) or manganese(II)/copper(II) nitrates in combination with (2,2,6,6-tetramethylpiperidin-1-yl)oxyl (TEMPO) selectively catalyze the oxidation of primary and secondary alcohols to the corresponding aldehydes and ketones.[15] Recently, copper(II) terpy complexes were used as

[a] *Department of Chemistry, Indian Institute of Technology Bombay, Mumbai 400076, India*
E-mail: rmv@chem.iitb.ac.in
http://www.chem.iitb.ac.in/~rmv/

Supporting information and ORCID(s) from the author(s) for this article are available on the WWW under https://doi.org/10.1002/ejic.201701064.

catalysts for alcohol oxidation reactions and offered good selectivity.[16]

Our laboratory has a longstanding interest in metallophosphate chemistry, and we have recently employed lipophilic mono- and diesters of phosphoric acid to generate a library of discrete and polymeric metallophosphates.[17] These metallophosphates find applications as single-source precursors for fine-particle ceramics and as molecular models to elucidate the mechanism of zeolite formation.[18] Although polymeric and cyclic manganese phosphates and phosphonates[19] as well as discrete or framework cobalt organophosphates are known,[20] there are no reports of dinuclear Mn^{II}, Co^{II}, and Ni^{II} complexes bridged by organophosphate ligands with terpy as an ancillary ligand, except the lone example of a dinuclear manganese terpyridine complex bridged by adenosine phosphate reported by Yashiro and co-workers.[21] On the basis of these facts and in continuation of our research into metallophosphates, we wish to report the synthesis of new dinuclear manganese, cobalt, and nickel phosphates with 4′-chloro-2,2′:6′,2″-terpyridine (Cl-terpy) and 2,6-diisopropylphenyl phosphate ($dippH_2$).

Results and Discussion

Synthesis and Spectral Characterization

The metal phosphates $[M(dipp)(Cl\text{-}terpy)(MeOH)]_2$ [M = Mn (**1**), Ni (**2**)] and $[Co(dippH)(Cl\text{-}terpy)(MeOH)(H_2O)]\cdot dippH$ (**3**) were synthesized through the reactions of equimolar quantities of $[M(OAc)_2\cdot 4H_2O]$ (M = Mn, Ni, and Co), $dippH_2$, and Cl-terpy in a $CH_3OH/CHCl_3$ solvent mixture (1:1 v/v) at room temperature (Scheme 1). In each case, the clear reaction mixture was left to stand at room temperature to yield the respective product as either single crystals or as a powder. The analytical and spectroscopic data were combined with single-crystal X-ray diffraction studies to identify the correct compositions and structures of the complexes. Complexes **1** and **2** exist as phosphate-bridged dimeric species both in solution and in the solid state. Although the cobalt complex **3** was isolated as a mononuclear species in the solid state, it exhibits a dimeric structure similar to those of **1** and **2** in solution (details below).

Compounds **1**–**3** are stable under ambient conditions and were characterized by various spectroscopic and analytical methods. The FTIR spectra of **1**–**3** show broad absorption bands at $\tilde{\nu} \approx 3400\ cm^{-1}$ for the OH group of the methanol molecules. The weak absorptions at $\tilde{\nu} \approx 3047$ and $2965\ cm^{-1}$ for **1**, 3035 and $2928\ cm^{-1}$ for **2**, and 3064 and $2961\ cm^{-1}$ for **3** correspond to the aromatic C–H stretching vibrations of the Cl-terpy and $dippH_2$ ligands. The absence of any absorption band at $\tilde{\nu} \approx 2350\ cm^{-1}$ for **1** and **2** indicates complete neutralization of all P–OH groups and, hence, no free P–OH groups in the $dippH_2$ ligand, whereas **3** shows a broad absorption band centered at $\tilde{\nu} \approx 2350\ cm^{-1}$, which indicates the presence of a residual P–OH group in the aryl phosphate ($dippH_2$) ligand in accordance with its molecular structure obtained by single-crystal studies (see below). The absorption bands at $\tilde{\nu} = 1084$, 1012, and $991\ cm^{-1}$ for **1**; 1124, 1049, and $1016\ cm^{-1}$ for **2**; and 1112, 1046, and $932\ cm^{-1}$ for **3** arise owing to the O–P–O stretching vibrations and M–O–P asymmetric and symmetric stretching vibrations, respectively (Figure S1).

The ESI-MS spectra of **1** and **2** exhibit peaks at $m/z = 1157$ and 1165, which correspond to $[M + H - 2MeOH]^+$ and, therefore, reveal the structural integrity of the dimeric structures in solution (Figure 1 and Supporting Information). Furthermore, compound **3**, which was isolated as a mononuclear complex in the solid state (see below), also exhibits a peak at $m/z = 1165$, which corresponds to the $[M - 2MeOH + H]^+$ ion (as for **1** and **2**) and, therefore, indicates that **3** has different structures in the solid state and in solution (Scheme 2).

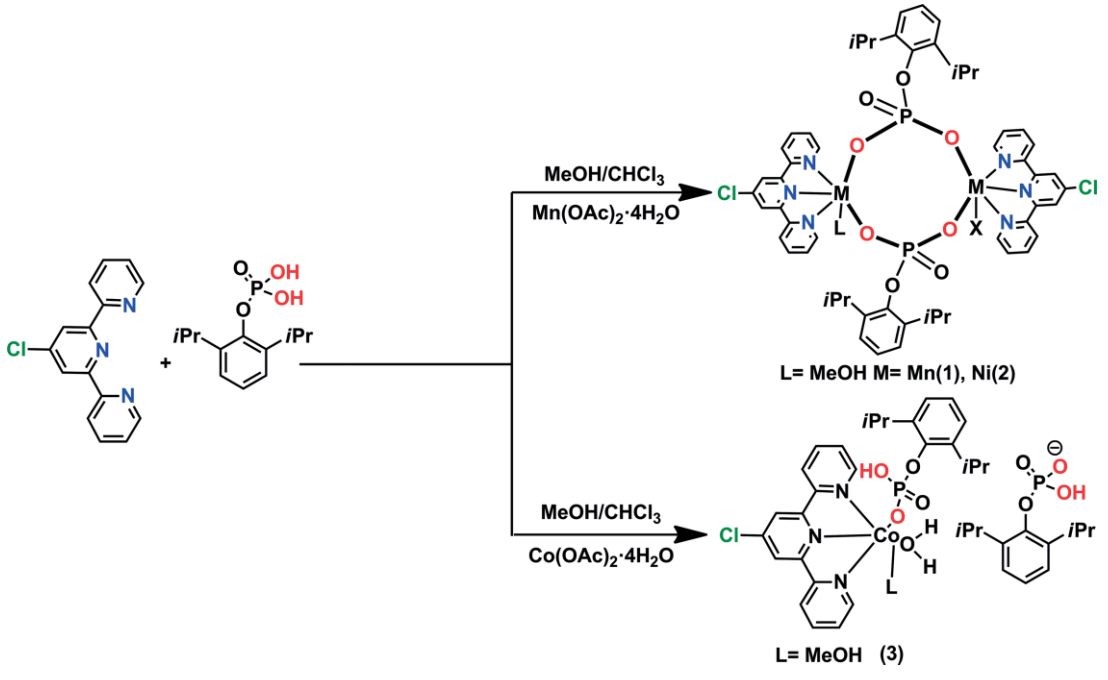

Scheme 1. Synthesis of **1**–**3**.

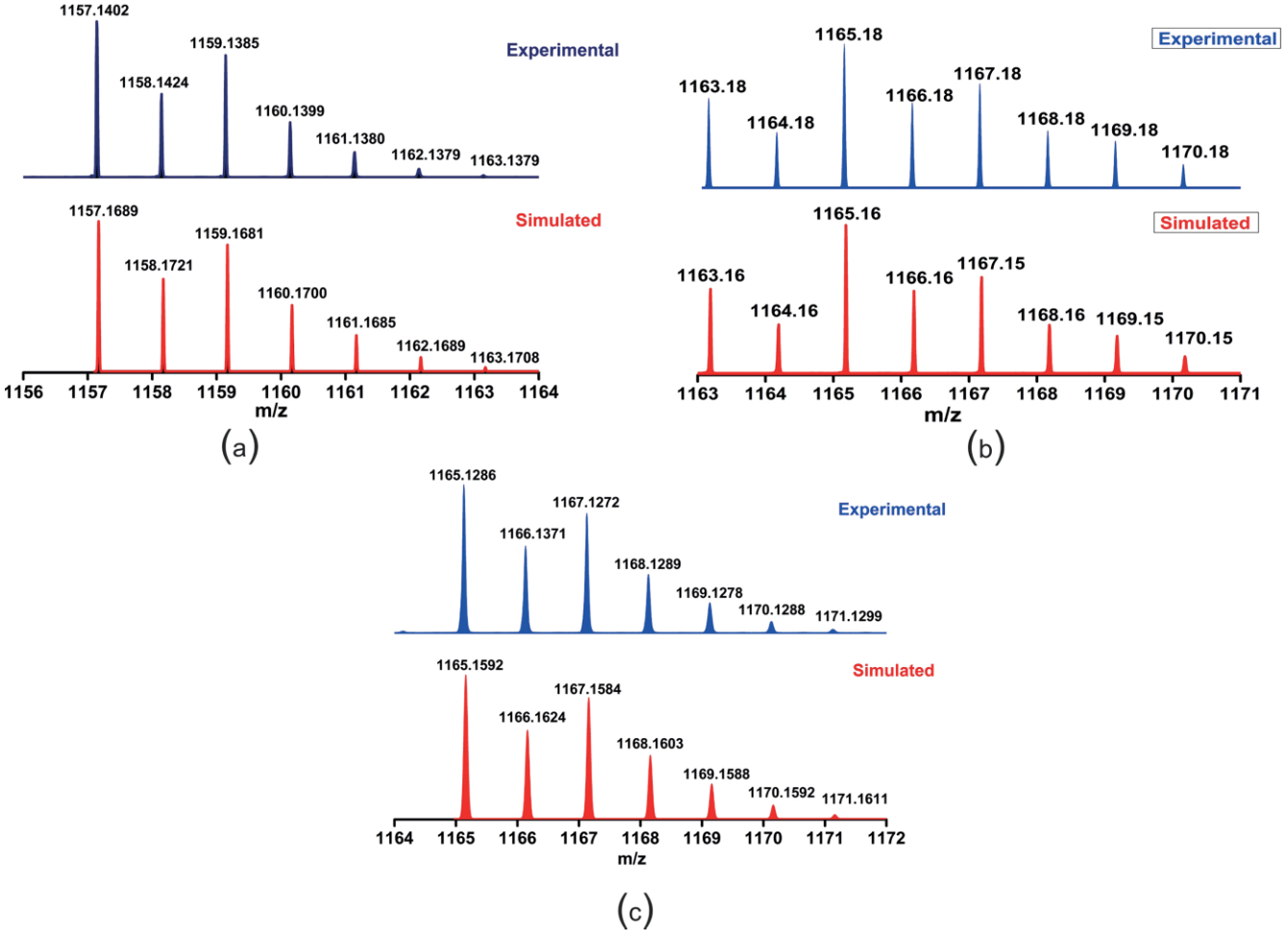

Figure 1. ESI-MS spectra showing the simulated and experimental isotope patterns for the $[M - 2MeOH + H]^+$ ions of **1**–**3**.

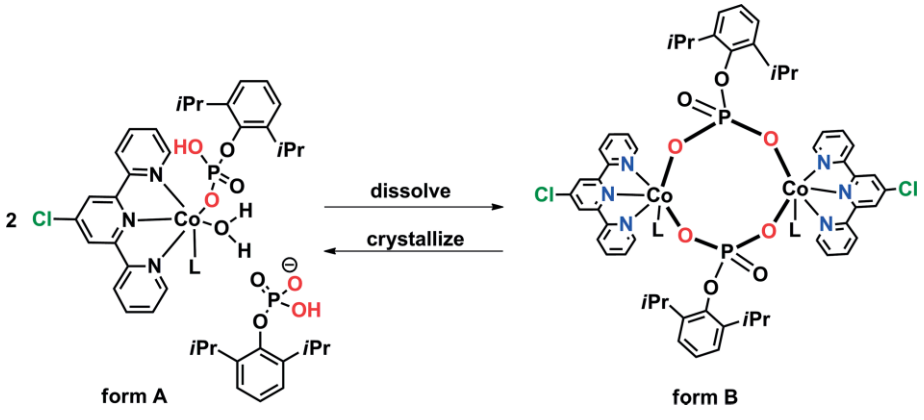

Scheme 2. Solid-state and solution structures of **3**.

Molecular Structure of 1

Compound **1** crystallizes in the triclinic space group $P\bar{1}$. A perspective view of the molecular structure is shown in Figure 2. Single-crystal X-ray diffraction studies revealed that **1** is dimeric with two Mn^{II} ions bridged by the phosphate ligand to form a cyclic manganese phosphate. The asymmetric unit of **1** contains one Mn^{II} ion, one doubly deprotonated aryl phosphate (dipp) ligand, a Cl-terpy ligand, and a coordinated methanol molecule. The Mn^{II} ion exhibits a distorted octahedral geometry, and the equatorial plane is occupied by the three nitrogen atoms (N1–N3) of the Cl-terpy ligand and an oxygen atom (O2) of the dipp ligand. The axial coordination sites are occupied by a coordinated methanol molecule (O5) and an oxygen atom of a second dipp ligand (O3).

Both the phosphate ligands are doubly deprotonated and bridge the Mn^{II} centers in a [2.110] fashion to form an eight-

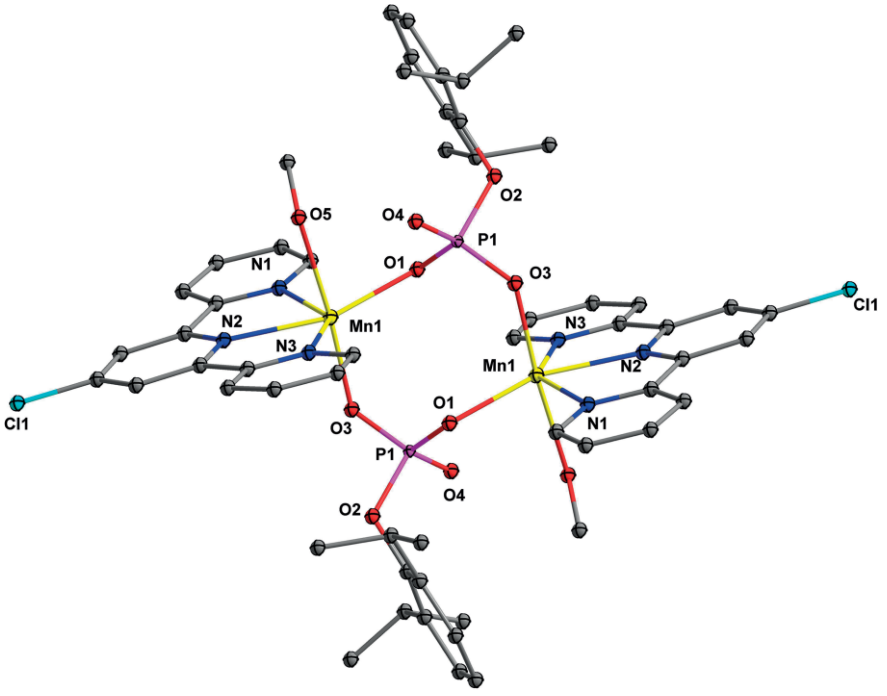

Figure 2. ORTEP representation of **1** at 50 % probability level. The hydrogen atoms were removed for clarity.

membered $Mn_2P_2O_4$ core.[22] The average P–O–M bond length of 1.521 Å is between the typical single and double bond lengths of phosphate ligands (P–OH 1.56 Å and P=O 1.48–1.50 Å). The average Mn–O bond length [2.086(2) Å] compares well with similar Mn–O bond lengths in other phosphonate and phosphate complexes.[19,23] Similarly, the average Mn–N bond length [2.282(2) Å] is comparable with the Mn–N bond lengths for similar Mn^{II} terpyridine complexes.[21,24] The average length of the Mn···P edges in the dinuclear complex is 3.230 Å, whereas the corresponding P···P distance is 4.591 Å. The Mn···Mn distance in **1** is 4.430 Å, which is smaller than those reported for dinuclear and tetranuclear Mn^{II} phosphates (4.472

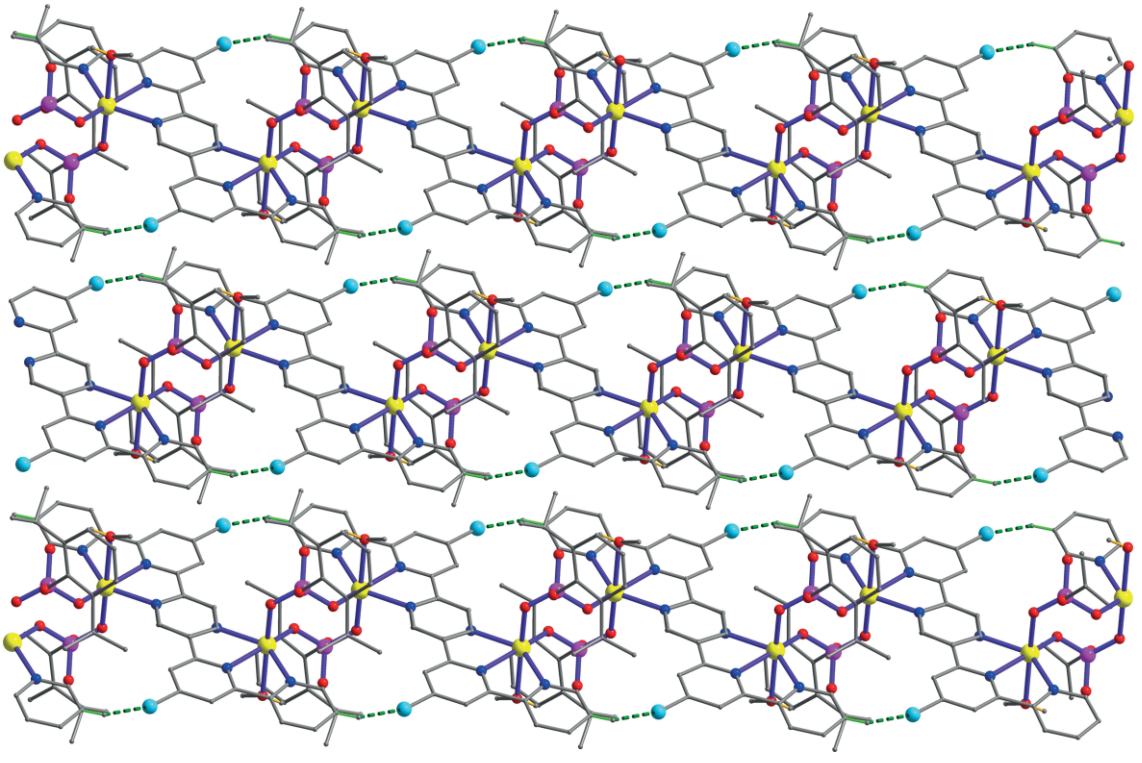

Figure 3. Polymeric 2D chain formed through C–H···Cl secondary interactions in **1**.

and 4.492 Å).[25] The chlorine atom of the Cl-terpy ligand is involved in C–H···Cl interactions with the C–H protons of another Cl-terpy ligand to form an interesting supramolecular aggregation that leads to the formation of 2D architectures (Figure 3).

Molecular Structure of 3

In contrast to the dinuclear structure expected for **3** from the ESI-MS studies (see above; Figure 1 and Scheme 2), the single-crystal X-ray diffraction studies revealed that **3** exists only as a mononuclear complex in the solid-state, as depicted in Figure 4. The asymmetric unit of **3** contains one Cl-terpy ligand, one dicationic Co^{II} ion, two monodeprotonated 2,6-diisopropylphenyl phosphate ligands (dippH, one coordinated, and the other occupying the lattice to maintain the electroneutrality), one coordinated water molecule, and one methanol molecule (Figure 4). The geometry around the Co^{II} ion is distorted octahedral; three nitrogen atoms from the chelating Cl-terpy ligand (N1–N3) and one oxygen atom of the aqua ligand (O5) occupy the equatorial plane, whereas the axial coordination sites are occupied by oxygen atoms from the dippH ligand (O1) and the coordinated methanol molecule (O6). The average Co–N [2.121(2) Å], P–O (Co) [1.499(2) Å], and Co–O bond lengths [2.069(2) Å] are comparable with those found in similar cobalt phosphates.[20,26] The negative charge on the lattice dippH phosphate is delocalized between O7 and O9; therefore, their bond metrics are comparable (P–O 1.498 Å).

The observed preference of **3** to exist in the mononuclear form, rather than the dinuclear structures exhibited by **1** and **2**, can be traced to structure-stabilizing H-bonding interactions. A quick comparison of the structures of **1** or **2** with that of **3** reveals a clear abundance of intra- and intermolecular O–H···O H-bonds in the latter (Figure 5). For example, strong hydrogen-bonding interactions occur between the protons of the coordinated water molecule (H5A and H5B) and the oxygen atom of coordinated methanol (O6) molecule and the oxygen atoms of the lattice dippH molecule (O9 and O3). Further, the free P–OH groups of the coordinated dippH ligand and the lattice dippH molecule also shows complimentary P–OH···O=P hydrogen bonding with each other. This pattern of hydrogen bonding leads to the formation of a cyclic dimeric structure, as shown in Figure 5. The formation of this dimeric structure, aided by the coordinated water molecule and the anionic lattice dippH molecule, is the probable driving force for the stabilization of a mononuclear complex for **3**. Further, the aryl rings of the Cl-

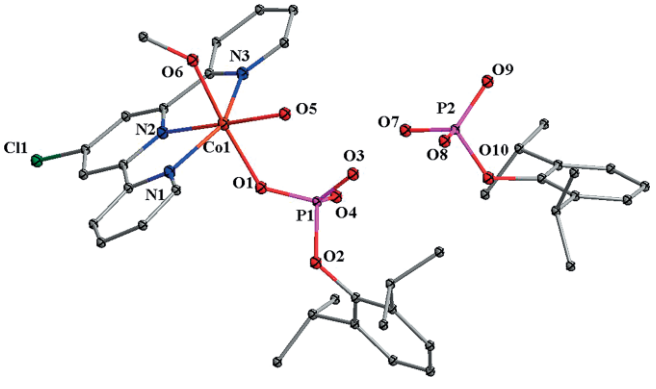

Figure 4. ORTEP representation of **3** at 50 % probability level. The hydrogen atoms were removed for clarity.

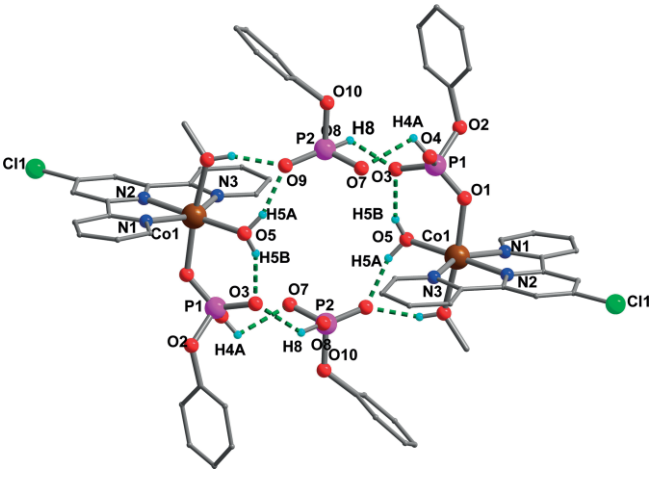

Figure 5. Cyclic dimer formation through O–H···O inter- and intramolecular hydrogen-bonding interactions in **3** (hydrogen atoms except those involved in hydrogen bonding and isopropyl groups of the phosphate ligands are omitted for clarity).

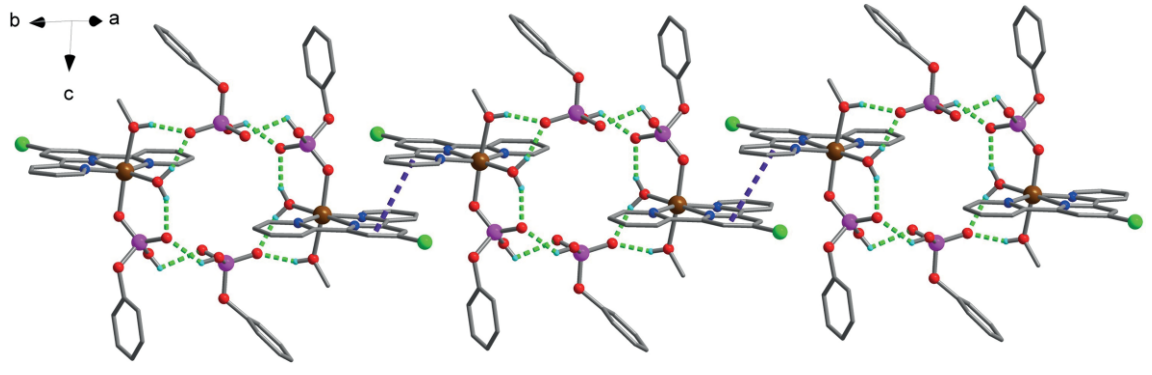

Figure 6. 1D polymeric chain formed through inter- and intramolecular hydrogen-bonding interactions and slipped π–π stacking between the adjacent benzene rings of the Cl-terpy ligands in **3** (hydrogen atoms except those involved in hydrogen bonding and isopropyl groups of the phosphate ligands are omitted for clarity).

terpy ligand show slipped π–π stacking among the adjacent molecules, which leads to the formation of one-dimensional polymeric chains (Figure 6).

Catalytic Studies

The catalytic properties of **1**–**3** in alcohol oxidation reactions were investigated. Initial optimization was performed for the oxidation of benzyl alcohol with the dimanganese phosphate **1** as the catalyst. To determine the suitable catalyst dose, five different catalyst loadings (0.125, 0.25, 0.375, 0.5, and 1 mol-%) were investigated, and the best conversion was obtained with 0.5 mol-% of catalyst; a total yield of 85 % was obtained, and 70 % of this was benzaldehyde (86 % selectivity). Although an increase of the catalyst loading to 0.5 mol-% enhances the product yield and selectivity (Figure 7), further increases (0.75 and 1 mol-%) led to reductions in both conversion (68 %) and benzaldehyde selectivity (44 %).

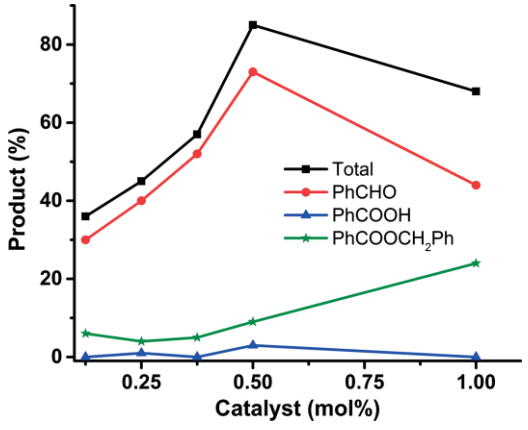

Figure 7. Effect of the catalyst dose on the product yield for benzyl alcohol oxidation catalyzed by **1** (benzyl alcohol: 10 mmol, CH_3CN: 10 mL, TBHP: 1 equiv., time: 4 h, temp.: 80 °C).

To determine the optimum reaction temperature, the oxidation of benzyl alcohol was performed at various temperatures, and the results are shown in Figure 8. Catalyst **1** exhibits the best catalytic activity (88 % product yield) at 100 °C, but the selectivity decreased at this temperature; however, when the reaction was performed at 80 °C with a similar catalyst loading, the product yield was 86 %, and the best benzaldehyde selectivity (73 %) was obtained. Thus, it can be concluded that temperatures beyond 80 °C enhance the product yield only marginally but at the cost of selectivity. Therefore, in terms of both conversion and selectivity, 80 °C was set as the optimum reaction temperature.

Five different solvents, namely, CH_3OH, CH_3CN, H_2O, hexane, and toluene, were screened to investigate the effect of the solvent on benzyl alcohol oxidation, and the results are shown in Figure 9. The maximum product yield (86 %) and selectivity (73 %) were observed for CH_3CN. The catalytic performance of **1** was also investigated under solvent-free conditions to make the process environmentally benign, but the product yield dropped to 65 % with only 13 % selectivity. Owing to this poor selectivity, solvent-free oxidation was ruled out.

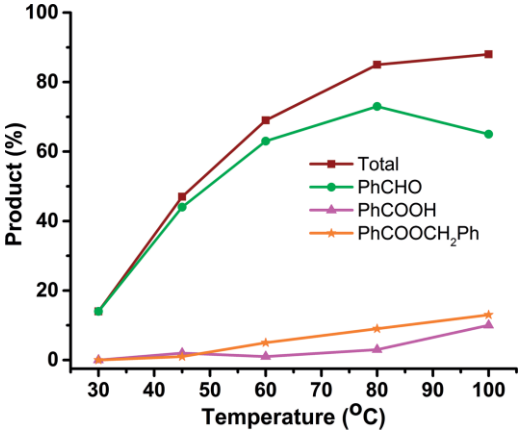

Figure 8. Effect of temperature on the product yield for benzyl alcohol oxidation catalyzed by **1** (catalyst: 0.5 mol-%, benzyl alcohol: 10 mmol, CH_3CN: 10 mL, TBHP: 1 equiv., time: 4 h).

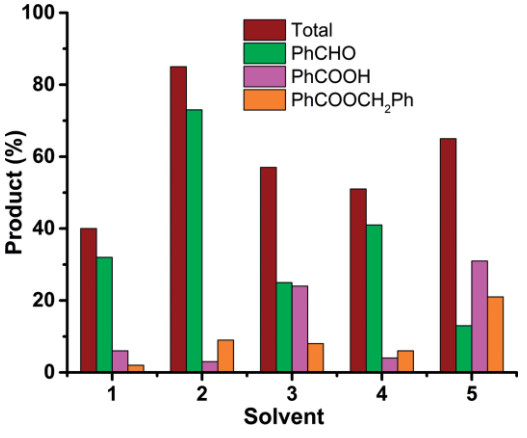

Figure 9. Effect of the solvent on the product yield for benzyl alcohol oxidation catalyzed by **1** (catalyst: 0.5 mol-%, $PhCH_2OH$: 10 mmol, solvent: 10 mL, TBHP: 1 equiv., time: 4 h, temp.: 80 °C. Solvents 1: CH_3OH; 2: CH_3CN; 3: H_2O; 4: hexane, 5: no solvent).

The optimum reaction time was standardized through the analysis of aliquots of the catalytic mixture at regular time intervals. The maximum product yield was obtained within 3 h, and the reactions performed for prolonged times did not show any significant differences for the conversion of benzyl alcohol (brown line, Figure 10). After 8 h of reaction, the selectivity decreases considerably owing to the further oxidation of the aldehyde to the acid and its ester. For these reasons, the optimum reaction time for maximum conversion and selectivity is 4 h.

Under these optimized conditions (catalyst amount, temperature, solvent, and time), the catalytic activities of catalysts **1**, **2**, and **3** for the oxidation of benzyl alcohol were investigated. As shown in Figure 11, the use of **1** as the catalyst resulted in better product yield (conversion) and product selectivity compared with those obtained with **2** and **3**.

The catalytic studies with complex **1** were extended to various alcohols, including a range of aliphatic, aromatic, primary, secondary, and heterocyclic alcohols. The results obtained are summarized in Table 1. It is evident from the data presented

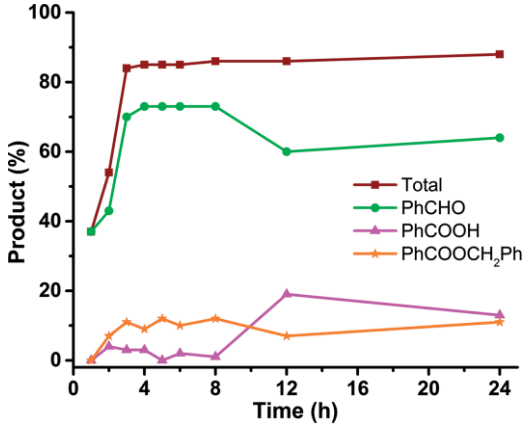

Figure 10. Effect of time on benzyl alcohol oxidation catalyzed by **1** (catalyst: 0.5 mol-%, $PhCH_2OH$: 10 mmol, CH_3CN: 10 mL, TBHP: 1 equiv., temp.: 80 °C).

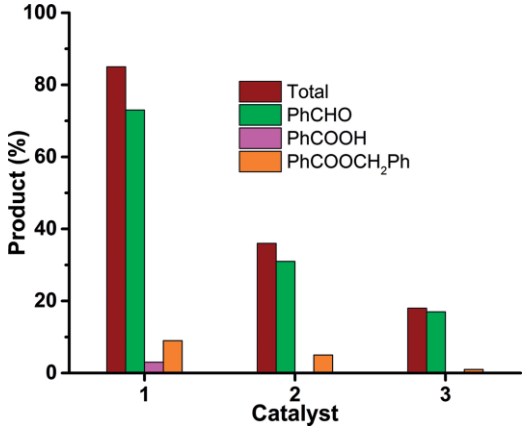

Figure 11. Comparison of the catalytic activities of catalysts **1**–**3** for the oxidation of benzyl alcohol (catalyst: 0.5 mol-%, $PhCH_2OH$: 10 mmol, CH_3CN: 10 mL, TBHP: 1 equiv., time: 4 h, temp.: 80 °C).

that better product yields are obtained for primary alcohols than for secondary alcohols. For example, 86 % product yield was observed for the oxidation of benzyl alcohol, whereas only 49 % product yield was obtained for the oxidation of 1-phenylethanol after 4 h. On the other hand, maximum selectivity (100 %) was reached for the secondary alcohol. If both primary and secondary alcohol groups are present in the substrate, the current catalytic system preferentially oxidizes the primary alcohol, as evidenced by the oxidation of glycerol. Furthermore, this catalytic system works better for alcohols with aromatic rings than for pure aliphatic alcohols, as evidenced by 1-pentanol oxidation (only 22 and 38 % conversion after 4 and 20 h, respectively).

Although Mn^{III} and Mn^{IV} complexes are well known as water oxidation catalysts,[27] a significant number of Mn^{II} complexes have been investigated for alcohol oxidations. The catalytic activities of previously reported Mn^{II} complexes for benzyl alcohol oxidation were compared with that of our Mn^{II} catalyst **1**, and the details are listed in Table 2.

Catalyst **1** demonstrated a superior catalytic activity than those all of the Mn^{II} complexes listed in Table 2 except for the mononuclear Mn^{II} complex reported by Boghaei and co-workers (Table 2, Entry 2). Although this mononuclear complex exhibits 100 % conversion and selectivity,[28] the oxidant used in this case was oxone, an unfavored oxidant for organic oxidation reactions. Furthermore, it should be noted that the non-heme Mn^{II} complex reported by Nam and co-workers (Table 2, Entry 3)[29] and a polymeric Mn^{II} complex reported by Bagherzadeh and co-workers (Table 2, Entry 6)[30] showed 100 % selectivity with reasonable conversion but only when harmful oxidants were employed as part of catalytic system. All of the other Mn^{II} complexes show lower activities than that of catalyst **1**, as evidenced by their poor conversions. The catalytic activity of catalyst **1** was also compared with those of free the Mn^{II} salts used in work of Huang and co-workers (Table 2, Entries 8 and 9)[32] in reactions under similar conditions (CH_3CN, TBHP, 80 °C), in which 5 mol-% of the catalysts resulted in poor conversions. Therefore, catalyst **1** is a better catalyst than many other earlier examples of Mn^{II} catalytic systems for the oxidation of benzyl alcohol. The kinetics of the oxidation reaction (plot of ln $[C_o/C_t]$ vs. time, C_o = initial concentration of benzyl alcohol, and C_t = concentration of benzyl alcohol at t) shows that the reaction reaches the saturation point after 4 h (see Figure S9). The turnover frequency (TOF) of catalyst **1** is 42.5 h^{-1}. Blank experiments exhibited very little activity in the absence of the catalyst or the oxidant.

Although the dimetallic Mn^{II} catalyst **1** seems to be a better option for benzyl alcohol oxidation than the already available homogeneous Mn^{II} catalysts, it has a few limitations. It would be promising if **1** showed better activity with water as the solvent or without the need for a solvent. We are working on these issues to overcome the limitations of this catalytic system and

Table 1. Oxidation of various alcohols catalyzed by **1**.[a]

Substrate	Aldehyde or ketone	Yield/selectivity [%]	Total yield [%]	TON[b]
Benzyl alcohol	benzaldehyde	73/86	85	170
2-phenylethanol	2-phenylacetaldehyde	11/100	11	22
1-phenylethan-1-ol	acetophenone	49/100	49	98
Diphenylmethanol	benzophenone	42/100	42	84
3-pyridinemethanol	3-pyridinecarbaldehyde	58/100	58	116
2,6-pyridinedimethanol	6-(hydroxymethyl)picolinaldehyde	17/35	48	96
	pyridine-2,6-dicarbaldehyde	31/65		
1-pentanol	1-pentanaldehyde	22/100	22	44
Glycerol	1-glyceraldehyde	44/100	44	88
Cyclohexanol	cyclohexanone	38/100	38	76

[a] Catalyst (0.5 mol-%), substrate (10 mmol), TBHP (1 equiv.), and acetonitrile (10 mL) at 80 °C. [b] Turnover number.

Table 2. Catalytic potential of **1** for the oxidation of benzyl alcohol in comparison to the earlier reported catalysts.

Entry	Catalyst	Products	Yield/selectivity [%]	Total [%]	Ref.
1	Catalyst **1**	PhCHO	73/86	85	this work
		PhCOOH	3/4		
		$PhCH_2COOPh$	9/10		
2	$[Mn(tptz)(Cl)_2(OH_2)]$[a]	PhCHO	100/100	100	[28]
3	$Mn(BPMCN)(CF_3SO_3)_2$[b]	PhCHO	70/100	70	[29]
4	$[Mn(C_6H_5COO)(H_2O)(phen)_2][ClO_4]\cdot CH_3OH$[c]	PhCHO	53.4/94	57	[14a]
		PhCOOH	3.6/6		
5	$[Mn_2(\mu\text{-}C_6H_5COO)_2(bipy)_4][ClO_4]_2$[d]	PhCHO	39.2/88	44.6	[14a]
		PhCOOH	5.4/12		
6	$[Mn(O_2CCH_2NH_2CH_2CO_2)_2(H_2O)_2]_n$	PhCHO	81/100	81	[30]
7	$[Mn(H_2O)_6](HL)_2\cdot 4H_2O$[e]	PhCHO	24/100	24	[31]
8	$MnCl_2\cdot 4H_2O$	PhCHO	20/100	20	[32]
9	$Mn(OAc)_2\cdot 4H_2O$	PhCHO	29/100	29	[32]

[a] tptz = 2,4,6-tris(2-pyridyl)-1,3,5-triazine. [b] BPMCN = *N*,*N*′-dimethyl-*N*,*N*′-bis(2-pyridylmethyl)cyclohexane-(1*R*,2*R*)-diamine. [c] phen = 1,10-phenanthroline. [d] bipy = 2,2′-bipyridyl. [e] HL = (*E*)-2-{2-(2-amino-1-cyano-2-oxoethylidene)hydrazinyl}benzenesulfonate.

make it more promising in terms of the choice of solvent and activity.

Conclusions

The Mn^{II}, Co^{II}, and Ni^{II} phosphates **1**–**3**, incorporating Cl-terpy and 2,6 diisopropylphenyl phosphate ligands, were synthesized and characterized by spectroscopic and analytical methods. Their molecular structures were confirmed by single-crystal X-ray diffraction studies. (Table 3) Through a combined solution ESI-MS and solid-state XRD study, it was established that the cobalt complex **3** exhibits dimeric and monomeric structures in these two states, respectively. Compounds **1**–**3** were employed as catalysts for benzyl alcohol oxidation reactions with *tert*-butyl hydroperoxide as the oxidant. The Mn^{II} compound **1** exhibits better catalytic activity in terms of both selectivity and substrate conversion compared with those of **2** and **3** under similar conditions. The fact that complexes **1**–**3** acts as efficient catalysts for the conversion of alcohols to ketones with environmentally benign TBHP as the oxidant highlights the importance of these terpyridine-based catalysts in alcohol oxidation reactions.

Table 3. Crystal data for **1** and **3**.

Compound	**1**	**3**
Identification code	GB-607	GB-495
Empirical formula	$C_{56}H_{64}Cl_2Mn_2N_6O_{10}P_2$	$C_{40}\ H_{52}ClCoN_3O_{10}P_2$
FW	1223.85	891.16
Temp. [K]	150(2)	100(2)
Crystal system	triclinic	triclinic
Space group	$P\bar{1}$	$P\bar{1}$
a [Å]	11.0154(3)	10.565(3)
b [Å]	11.1189(4)	12.911(3)
c [Å]	13.9568(4)	17.085(3)
α [°]	90.187(2)	72.194(10)
β [°]	109.891(3)	73.710(11)
γ [°]	116.368(3)	85.974(15)
V [Å^3]	1415.81(9)	2129.5(9)
Z	1	2
D(calcd.) [Mg/cm^3]	1.435	1.390
μ [mm^{-1}]	0.660	0.600
θ range [°]	2.216 to 24.999	2.603 to 25.000
Reflections collected	10829	16021
Independent reflections	4970	7432
GOF	1.033	1.117
R_1 [$I_0 > 2\sigma(I_0)$]	0.0372	0.0554
wR_2 (all data)	0.1004	0.1448

Experimental Section

Materials and Methods: Solvents were purified by standard procedures before use. The starting materials $[M(OAc)_2\cdot 4H_2O]$ (M = Mn, Co, Ni; s.d. Fine) and Cl-terpy (Sigma–Aldrich) were procured from commercial sources and used as received. $DippH_2$ was synthesized by a literature procedure.[33] 70 % aqueous TBHP was procured from Spectrochem. All of the reactions were performed in the open atmosphere without any precautions to exclude air or moisture. The melting points were measured with the compounds in glass capillaries. The infrared spectra were obtained with a Perkin–Elmer Spectrum One FTIR spectrometer with the samples as diluted KBr discs. Microanalyses were performed with a Thermo Finnigan (FLASH EA 1112) microanalyzer. Thermogravimetric analyses were performed with a Perkin–Elmer Pyris thermal analysis system with the samples under a stream of nitrogen gas at a heating rate of 10 °C/min. The ESI-MS studies were performed with a Bruker MaXis impact mass spectrometer. The UV/Vis spectra were recorded with a Varian Cary Bio 100 spectrophotometer.

$[M(dipp)(Cl\text{-}terpy)]_2$ [M = Mn (1), Ni (2)] and $[Co(dippH)(Cl\text{-}terpy)(MeOH)(H_2O)]\cdot(dippH)$ (3): To a stirred solution of Cl-terpy (0.081 g, 0.3 mmol) and $dippH_2$ (0.077 g, 0.3 mmol) in a $CH_3OH/CHCl_3$ (1:1 v/v) solvent mixture, $[M(OAc)_2\cdot 4H_2O]$ (M = Mn, 0.073 g, 0.3 mmol; M=Co, 0.074 g, 0.3 mmol; M = Ni, 0.075 g,0.3 mmol) in CH_3OH was added under constant stirring at room temperature. The clear solution obtained in each case was filtered and kept for crystallization at room temperature through the slow evaporation of the solvent. Yellow and red single crystals of **1** and **3** were obtained in one week, whereas **2** was obtained as a green crystalline precipitate.

1: M.p. >250 °C. Yield 0.203 g (56 % based on $dippH_2$). $C_{56}H_{62}Cl_2Mn_2N_6O_{10}P_2$ (1221.87): calcd. C 55.05, H 5.11, N 6.88; found C 54.00, H 4.82, N 6.66. FTIR (KBr disc): $\tilde{\nu}$ = 3410 (br), 3047 (s), 2965 (vs), 2390 (br), 1084 (s), 1012 (s), 991 (s), 899 (s), 761 (s) cm^{-1}. ESI-MS: calcd. for $C_{54}H_{54}N_6O_8P_2Mn_2Cl_2$ $[M - 2MeOH + H]^+$ 1157; found 1157.

2: M.p. >250 °C. Yield 0.217 g (59 % based on $dippH_2$). $C_{56}H_{62}Cl_2N_6Ni_2O_{10}P_2$ (1229.41): calcd. C 54.71, H 5.08, N 6.84; found

C 53.98, H 5.80, N 4.74. FTIR (KBr disc): $\tilde{\nu}$ = 3410 (br), 3055 (s), 2928 (vs), 2350 (br), 112 (s), 1049 (s), 1016 (s), 881 (vs), 793 (s), 741 (s), 580 (s) cm^{-1}. ESI-MS: calcd. for $C_{54}H_{54}N_6O_8P_2Ni_2Cl_2$ $[M + H]^+$ 1165; found 1165.

3: M.p. >250 °C. Yield 0.130 g (49 % based on $dippH_2$). $C_{40}H_{52}ClCoN_3O_{10}P_2$ (891.20): calcd. C 53.91, H 5.88, N 4.72; found C 53.23, H 4.92, N 6.56. FTIR (KBr disc): $\tilde{\nu}$ = 3410 (br), 2963 (vs), 2390 (br), 1592 (s), 1162 (s), 933 (s), 925 (vs), 769 (s), 741 (s), 580 (s), 538 (s) cm^{-1}. ESI-MS: calcd. for $C_{54}H_{54}N_6O_8P_2Co_2Cl_2$ $[M + H]^+$ 1165; found 1165.

Oxidation of Alcohols: Before the reaction, a two-necked flask was equipped with a magnetic bar, and then the catalyst (0.5 mol-%), CH_3CN (10 mL), substrate (alcohol, 10 mmol), and 70 % aqueous TBHP (1 equiv.) were added successively. The resultant catalytic mixture was heated under reflux at 80 °C for 4 h. Aliquots were removed and diluted with ethyl acetate for the GC–MS analysis. An Agilent Technologies 5975C GC–MS system was used to monitor the oxidation of the alcohols. Two separate blank experiments (one without oxidant and one without catalyst) were also performed with all other conditions unaltered.

Single-Crystal X-ray Diffraction Studies: The single-crystal X-ray diffraction data for **1** and **3** were recorded with a Rigaku Saturn 724+ CCD diffractometer with a Mo-K_α radiation source (λ = 0.71075 Å) at 150 K. The crystal Clear-SM Expert software was used for the data collection, and the data integration and indexing were performed with the CrysAlisPro software suite.[34] The WinGX module was used to perform all of the calculations.[35] The structures were solved by direct methods with SIR-92.[36] The final structure refinements were performed by full least-squares methods on F^2 with SHELXL-2014.[37] All non-hydrogen atoms were refined anisotropically. The hydrogen atoms were refined isotropically as rigid atoms in their idealized locations.

CCDC 1571740 (for **1**) and 1571741 (for **3**) contain the supplementary crystallographic data for this paper. These data can be obtained free of charge from The Cambridge Crystallographic Data Centre.

Acknowledgments

R. M. is grateful to SERB, New Delhi for a JC Bose Fellowship (SB/S2/JCB-85/2014), through which this research was carried out. G. B. thanks the University Grants Commission (UGC), New Delhi for providing a fellowship. R. A. thanks the Department of Science and Technology (DST), SERB for a National Postdoctoral Fellowship (NPDF/ 2016/00037).

Keywords: Phosphate ligands · Alcohols · Oxidation · Homogeneous catalysis · Structure elucidation

[1] a) R. A. Sheldon, J. K. Kochi, *Metal-Catalyzed Oxidations of Organic Compounds: Mechanistic Principles*, Academic Press, New York, **1981**; b) S. Debnath, S. K. Saxena, V. Nagabhatla, *Catal. Commun.* **2016**, *84*, 129–133; c) D. I. Enache, J. K. Edwards, P. Landon, B. Solsona-Espriu, A. F. Carley, A. A. Herzing, M. Watanabe, C. J. Kiely, D. W. Knight, G. J. Hutchings, *Science* **2006**, *311*, 362–365; d) S. Verma, R. N. Baig, M. N. Nadagouda, R. S. Varma, *ACS Sustainable Chem. Eng.* **2016**, *4*, 1094–1098; e) C. Bai, A. Li, X. Yao, H. Liu, Y. Li, *Green Chem.* **2016**, *18*, 1061–1069; f) Y. Yan, X. Tong, K. Wang, X. Bai, *Catal. Commun.* **2014**, *43*, 112–115; g) X. Li, R. Cao, Q. Lin, *Catal. Commun.* **2015**, *69*, 5–10.

[2] A. Dijksman, A. Marino-González, A. Mairata i Payeras, I. W. Arends, R. A. Sheldon, *J. Am. Chem. Soc.* **2001**, *123*, 6826–6833.

[3] a) I. Kani, M. Kurtca, *Turk. J. Chem.* **2012**, *36*, 827–840; b) P. Gallezot, *Catal. Today* **1997**, *37*, 405–418; c) M. Hayashi, K. Yamada, S.-z. Nakayama, H. Hayashi, S. Yamazaki, *Green Chem.* **2000**, *2*, 257–260; d) M. Besson, P. Gallezot, *Catal. Today* **2000**, *57*, 127–141.

[4] V. R. Choudhary, P. A. Chaudhari, V. S. Narkhede, *Catal. Commun.* **2003**, *4*, 171–175.

[5] J. Mobley, M. Crocker, *RSC Adv.* **2015**, *5*, 65780–65797.

[6] D. Wang, D. Astruc, *Chem. Soc. Rev.* **2017**, *46*, 816–854.

[7] a) Y. Kwon, S. C. Lai, P. Rodriguez, M. T. Koper, *J. Am. Chem. Soc.* **2011**, *133*, 6914–6917; b) C. Parmeggiani, F. Cardona, *Green Chem.* **2012**, *14*, 547–564.

[8] a) D. Toledo, G. Ahumada, C. Manzur, T. Roisnel, O. Peña, J.-R. Hamon, J.-Y. Pivan, Y. Moreno, *J. Mol. Struct.* **2017**, *1146*, 213–221; b) M. Wang, T. Weyhermüller, E. Bill, S. Ye, K. Wieghardt, *Inorg. Chem.* **2016**, *55*, 5019–5036; c) J. Grau, R. F. Brissos, J. Salinas-Uber, A. B. Caballero, A. Caubet, O. Roubeau, L. Korrodi-Gregório, R. Pérez-Tomás, P. Gamez, *Dalton Trans.* **2015**, *44*, 16061–16072; d) G. Zhang, H. Zeng, J. Wu, Z. Yin, S. Zheng, J. C. Fettinger, *Angew. Chem. Int. Ed.* **2016**, *55*, 14369–14372; *Angew. Chem.* **2016**, *128*, 14581–14584; e) J.-J. Liu, Y.-J. Lin, G.-X. Jin, *Organometallics* **2014**, *33*, 1283–1290; f) W.-Y. Zhang, Y.-F. Han, L.-H. Weng, G.-X. Jin, *Organometallics* **2014**, *33*, 3091–3095; g) E. C. Constable, G. Zhang, C. E. Housecroft, M. Neuburger, J. A. Zampese, *CrystEngComm* **2009**, *11*, 2279–2281; h) G. Zhang, J. Tan, Y. Z. Zhang, C. Ta, S. Sanchez, S.-Y. Cheng, J. A. Golen, A. L. Rheingold, *Inorg. Chim. Acta* **2015**, *435*, 147–152.

[9] E. C. Constable, G. Zhang, E. Coronado, C. E. Housecroft, M. Neuburger, *CrystEngComm* **2010**, *12*, 2139–2145.

[10] a) A. Winter, G. R. Newkome, U. S. Schubert, *ChemCatChem* **2011**, *3*, 1384–1406; b) I. Eryazici, C. N. Moorefield, G. R. Newkome, *Chem. Rev.* **2008**, *108*, 1834–1895; c) S. Ghosh, O. Mendoza, L. Cubo, F. Rosu, V. Gabelica, A. J. White, R. Vilar, *Chem. Eur. J.* **2014**, *20*, 4772–4779.

[11] J. Limburg, J. S. Vrettos, L. M. Liable-Sands, A. L. Rheingold, R. H. Crabtree, G. W. Brudvig, *Science* **1999**, *283*, 1524–1527.

[12] a) H. Yamazaki, S. Igarashi, T. Nagata, M. Yagi, *Inorg. Chem.* **2012**, *51*, 1530–1539; b) H. Yamazaki, T. Ueno, K. Aiso, M. Hirahara, T. Aoki, T. Nagata, S. Igarashi, M. Yagi, *Polyhedron* **2013**, *52*, 455–460; c) H. Lv, J. A. Rudd, P. F. Zhuk, J. Y. Lee, E. C. Constable, C. E. Housecroft, C. L. Hill, D. G. Musaev, Y. V. Geletii, *RSC Adv.* **2013**, *3*, 20647–20654.

[13] a) H. Chen, M.-N. Collomb, C. Duboc, G. Blondin, E. Rivière, J. Faller, R. H. Crabtree, G. W. Brudvig, *Inorg. Chem.* **2005**, *44*, 9567–9573; b) B. Machura, J. Palion, J. Mroziński, B. Kalińska, M. Amini, M. Najafpour, R. Kruszynski, *Polyhedron* **2013**, *53*, 132–143; c) S. Khan, K. R. Yang, M. Z. Ertem, V. S. Batista, G. W. Brudvig, *ACS Catal.* **2015**, *5*, 7104–7113.

[14] a) I. Kani, S. Bolat, *Appl. Organomet. Chem.* **2016**, *30*, 713–721; b) B. Choudary, M. L. Kantam, A. Rahman, C. Reddy, K. K. Rao, *Angew. Chem. Int. Ed.* **2001**, *40*, 763–766; *Angew. Chem.* **2001**, *113*, 785; c) G. J. Britovsek, J. England, S. K. Spitzmesser, A. J. White, D. J. Williams, *Dalton Trans.* **2005**, 945–955.

[15] A. Cecchetto, F. Fontana, F. Minisci, F. Recupero, *Tetrahedron Lett.* **2001**, *42*, 6651–6653.

[16] a) Z. Ma, L. Wei, E. C. Alegria, L. M. Martins, M. F. C. G. da Silva, A. J. Pombeiro, *Dalton Trans.* **2014**, *43*, 4048–4058; b) K. Czerwińska, B. Machura, S. Kula, S. Krompiec, K. Erfurt, C. Roma-Rodrigues, A. R. Fernandes, L. S. Shul'pina, N. S. Ikonnikov, G. B. Shul'pin, *Dalton Trans.* **2017**, *46*, 9591–9604.

[17] a) A. A. Dar, S. K. Sharma, R. Murugavel, *Inorg. Chem.* **2015**, *54*, 4882–4894; b) A. A. Dar, G. A. Bhat, R. Murugavel, *Inorg. Chem.* **2016**, *55*, 5180–5190.

[18] a) S. K. Gupta, A. C. Kalita, A. A. Dar, S. Sen, G. N. Patwari, R. Murugavel, *J. Am. Chem. Soc.* **2017**, *139*, 59–62; b) R. Murugavel, M. Sathiyendiran, M. G. Walawalkar, *Inorg. Chem.* **2001**, *40*, 427–434; c) R. Pothiraja, M. Sathiyendiran, R. J. Butcher, R. Murugavel, *Inorg. Chem.* **2004**, *43*, 7585–7587.

[19] R. Pothiraja, P. Rajakannu, P. Vishnoi, R. J. Butcher, R. Murugavel, *Inorg. Chim. Acta* **2014**, *414*, 264–273.

[20] S. K. Gupta, S. Kuppuswamy, J. P. S. Walsh, E. J. L. McInnes, R. Murugavel, *Dalton Trans.* **2015**, *44*, 5587–5601.

[21] M. Yashiro, M. Higuchi, M. Komiyama, Y. Ishii, *Bull. Chem. Soc. Jpn.* **2003**, *76*, 1813–1817.

[22] G. A. Bhat, P. Vishnoi, S. K. Gupta, R. Murugavel, *Inorg. Chem. Commun.* **2015**, *59*, 84–87.

[23] T. Kuroda-Sowa, T. Handa, T. Kotera, M. Maekawa, M. Munakata, H. Miyasaka, M. Yamashita, *Chem. Lett.* **2004**, *33*, 540–541.
[24] M. Sathiyendiran, R. Murugavel, *Inorg. Chem.* **2002**, *41*, 6404–6411.
[25] R. Pothiraja, M. Sathiyendiran, R. J. Butcher, R. Murugavel, *Inorg. Chem.* **2005**, *44*, 6314–6323.
[26] R. Murugavel, M. G. Walawalkar, M. Dan, H. W. Roesky, C. N. R. Rao, *Acc. Chem. Res.* **2004**, *37*, 763–774.
[27] a) M. K. Brown, M. M. Blewett, J. R. Colombe, E. Corey, *J. Am. Chem. Soc.* **2010**, *132*, 11165–11170; b) C. Zondervan, R. Hage, B. L. Feringa, *Chem. Commun.* **1997**, 419–420; c) Z. Li, Z. H. Tang, X. X. Hu, C. G. Xia, *Chem. Eur. J.* **2005**, *11*, 1210–1216; d) G. B. Shul'pin, G. Süss-Fink, L. S. Shul'pina, *J. Mol. Catal. A* **2001**, *170*, 17–34; e) R. Ruiz, A. Aukauloo, Y. Journaux, I. Fernández, J. R. Pedro, A. L. Roselló, B. Cervera, I. Castro, M. C. Muñoz, *Chem. Commun.* **1998**, 989–990.
[28] M. M. Najafpour, M. Amini, M. Bagherzadeh, D. M. Boghaei, V. McKee, *Trans. Met. Chem.* **2010**, *35*, 297–303.
[29] K. Nehru, S. J. Kim, I. Y. Kim, M. S. Seo, Y. Kim, S.-J. Kim, J. Kim, W. Nam, *Chem. Commun.* **2007**, 4623–4625.
[30] M. Bagherzadeh, M. Amini, D. M. Boghaei, M. M. Najafpour, V. McKee, *Appl. Organomet. Chem.* **2011**, *25*, 559–563.
[31] K. T. Mahmudov, M. Sutradhar, L. M. Martins, M. F. C. G. da Silva, A. Ribera, A. V. Nunes, S. I. Gahramanova, F. Marchetti, A. J. Pombeiro, *RSC Adv.* **2015**, *5*, 25979–25987.
[32] H. y. Sun, Q. Hua, F. f. Guo, Z. y. Wang, W. x. Huang, *Adv. Synth. Catal.* **2012**, *354*, 569–573.
[33] G. M. Kosolapoff, C. K. Arpke, R. W. Lamb, H. Reich, *J. Chem. Soc. C* **1968**, 815–818.
[34] *CrysAlisPro*, Oxford Diffraction Ltd, Abingdon, **2006**.
[35] L. Farrugia, *J. Appl. Crystallogr.* **1999**, *32*, 837–838.
[36] A. Altomare, G. Cascarano, C. Giacovazzo, A. Guagliardi, *J. Appl. Crystallogr.* **1993**, *26*, 343–350.
[37] G. M. Sheldrick, *Acta Crystallogr., Sect. C* **2015**, *71*, 3–8.

Received: September 5, 2017

